

Frequency-dependent polarization-angle-phase-shift in the microwave-induced magnetoresistance oscillations

Han-Chun Liu,¹ Tianyu Ye,¹ W. Wegscheider,² and R. G. Mani¹

¹*Department of Physics and Astronomy, Georgia State University, Atlanta, Georgia 30303*

²*Laboratorium für Festkörperphysik, ETH Zürich, CH-8093 Zürich, Switzerland*

(Dated: 15 July 2021)

Linear polarization angle, θ , dependent measurements of the microwave radiation-induced oscillatory magnetoresistance, R_{xx} , in high mobility GaAs/AlGaAs 2D electron devices have shown a θ dependence in the oscillatory amplitude along with magnetic field, frequency, and extrema-dependent phase shifts, θ_0 . Here, we suggest a microwave frequency dependence of $\theta_0(f)$ using an analysis that averages over other smaller contributions, when those contributions are smaller than estimates of the experimental uncertainty.

I. INTRODUCTION

The quasi two-dimensional electron system (2DES) in high mobility GaAs/AlGaAs heterostructures has served to identify a new type of zero-resistance state in the 2DES, one which occurs at high filling factors or low magnetic fields under microwave photo-excitation.^{1,2} Such zero-resistance states have been fascinating in part because they could help to point out the necessary conditions for obtaining vanishing resistance in the 2DES in a magnetic field. The associated oscillatory effect is also interesting from the application perspective since it could lead to new approaches for a frequency and power sensitive radiation detector in the microwave and terahertz bands, for a large number of applications.³⁻⁵

Numerous experimental^{1,2,5-36} and theoretical³⁷⁻⁷⁵ works about the radiation-induced magnetoresistance oscillations (RIMO) and associated zero-resistance states have been published over the past decade. At the present, it is understood that RIMOs are 1/4-cycle phase-shifted in $1/B$, and the oscillatory minima occur in R_{xx} vs. B plots broadly about $B = [4/(4j+1)]B_f$, where $B_f = 2\pi fm^*/e$, f is the microwave frequency, m^* is the effective electron mass in GaAs and $j = 1, 2, 3, \dots$. The theoretically proposed physical mechanisms for RIMOs include the displacement model^{37,39}, the nonparabolicity model⁴⁰, the inelastic model⁵⁰ and the radiation-driven electron-orbit model^{48,53}. These different theories have suggested dissimilar behavior of some physical properties such as, for example the polarization-angle-dependence and the power-dependence of the RIMOs. As a result, an interesting issue concerns the sensitivity of the RIMOs to the polarization angle of linearly polarized microwaves. Early linear microwave polarization sensitivity work carried out on L-shaped samples⁹ showed that the the frequency and the phase of RIMOs are insensitive to the linear polarization angle of the microwaves. Later work indicated that RIMOs were insensitive to circularly and linearly polarized microwaves in square-shaped samples in a quasi-optical measurement¹². More recently, a polarization-angle-dependence in the amplitude of RIMOs has been demonstrated^{25,26,36}. The results were roughly consistent with the predictions of the displacement model, the nonparabolicity model, and

the radiation-driven electron-orbit model for $\gamma < \omega$, where γ is damping factor and $\omega = 2\pi f$.^{37,39,40,48,53,68} Finally, Ramanayaka *et al.* showed that the R_{xx} varied sinusoidally vs. θ at low microwave power, following the empirical relation $R_{xx}(\theta) = A \pm C \cos^2(\theta - \theta_0)$, where θ is microwave polarization angle, θ_0 is phase shift, and the plus and minus signs corresponded to the oscillatory maxima and minima, respectively.²⁶ The results suggested both a f -dependence and a B -dependence in θ_0 , although the phase shifts did not appear to be systematically responsive to any experimental parameters. These studies indicated that the observed phase shifts required further experimental investigation.

Thus, we extract the frequency dependence of the phase shift in the R_{xx} vs. θ results by applying an analysis that averages over other smaller contributions, when those contributions are smaller than estimates of the experimental uncertainty. The results suggest a non-vanishing frequency dependence in the phase shift, i.e., $\theta_0 = \theta_0(f)$, over the frequency interval $32 \leq f \leq 50$ GHz.

II. EXPERIMENT AND RESULTS

The experimental setup for the polarization-orientation measurements is shown in Fig. 1(a). Linearly polarized microwaves are generated by an antenna inside a rotatable microwave launcher, and they are transmitted via a cylindrical waveguide to the sample. The samples consist of 400- μm -wide Hall bar with alloyed gold-germanium contacts fabricated from GaAs/AlGaAs heterojunctions with a 2DES with carrier density $\approx 2.7 \times 10^{11} \text{cm}^{-2}$ and mobility $\approx 8 \times 10^6 \text{cm}^2 \cdot \text{V}^{-1} \cdot \text{s}^{-1}$. The samples are immersed in pumped liquid helium to maintain a temperature of 1.5 K during the measurements. Standard four-terminal lock-in techniques are utilized to measure the diagonal resistance R_{xx} . Finally, the polarization angle θ is defined as the angle between the microwave electric field E and the Hall bar axis. Thus, in experiment, the gradual increase of θ from 0° to 360° is achieved by rotating the microwave launcher.

At the outset to the experiment, a power detector is connected to a power meter and placed at the end of

cylindrical waveguide, see Fig. 1(c) inset. This power detector is sensitive to the radiation field along its preferred axis. The orientation of this detector is fixed parallel to the antenna, setting $\theta = 0^\circ$. Then, the antenna is turned from 0° to 360° at 5° increment for a number of different frequencies, f , from 32 GHz to 50 GHz, to characterize the linear polarization angle of the microwaves at the bottom of the waveguide sample holder. Fig. 1(c) shows the normalized detected power as a function of θ at 40.791 GHz. As expected for linearly polarized microwaves, the detected power varies sinusoidally with θ , and this sinusoidal curve can be described by $P = A + C \cos^2(\theta - \theta_0)$, where P is the detected power, A is the dark response without microwaves, and C is the amplitude of cosine square function. The cosine square function has been used here because the microwave power is proportional to the square of the microwave electric field. Such data fits to this sinusoidal function were used to extract a phase shift, θ_0 , in the absence of a sample to characterize the polarization angle in the measurement setup. Fig. 1(c) demonstrates good fit between detector response and the sinusoidal function, as the fit indicates that $\theta_0 = 0.2^\circ \pm 0.3^\circ$ at $f = 40.791$ GHz. This same method was used to extract θ_0 at a number of frequencies. These fit-extracted θ_0 of the bare sample holder plus detector have been plotted as a function of f in Fig. 1(d), which indicates that $-8^\circ \leq \theta_0 \leq 6^\circ$ for $32 \leq f \leq 50$ GHz. Here, one expects that $\theta_0 = 0$ if the microwave antenna is well aligned with the microwave detector when the $\theta = 0$ condition is defined at each f . Thus, the observed spread in these θ_0 , which is $\approx 14^\circ$, is attributed to experimental issues such as misalignment and readout errors.

In the next experimental phase, B -field sweeps of R_{xx} with microwave (photo-excited R_{xx}) and without microwave excitation (dark R_{xx}) were carried out from -0.3 T to 0.3 T at a number of frequencies. Figs. 2(a), and 2(b) both show photo-excited and dark R_{xx} vs B with $f = 32.5$ GHz, $P = 0.63$ mW at $\theta = 0^\circ$ for $0 \leq B \leq 0.3$ T. Here, Fig. 2(a) (labeled with the superscript sign of L) represents measurements from the contact pair on the left side of the Hall bar, while Fig. 2 (b) (labeled with the superscript sign of R) represents measurements from the right side of the Hall bar. Both Fig. 2(a) and 2(b) exhibit perceptible RIMOs below 0.15 T. Thus, in Fig. 2(a) and (b), the predominant oscillatory extrema of RIMOs have been labeled as $P1+$, $V1+$, and $P2+$, to indicate the first peak, the first valley, and the second peak, respectively, of RIMOs for $B \geq 0$. Fig. 2(c)-(h) display dark and photo-excited R_{xx} as a function of θ at fixed B corresponding to $P1+^L$, $P1+^R$, $V1+^L$, $V1+^R$, $P2+^L$, and $P2+^R$. Note that the photo-excited R_{xx} varies sinusoidally with θ , and the dark R_{xx} maintains a constant value vs. θ .

The phase shifts θ_0 in the R_{xx} vs. θ data are extracted by fitting to $R_{xx} = A \pm C \cos^2(\theta - \theta_0)$, with "+" sign for peaks and "-" sign for valleys. Associated fit curves are also shown in Fig. 2(c)-(h). To compare these θ_0 , let us begin by focusing upon Fig. 2(c) ($P1+^L$)

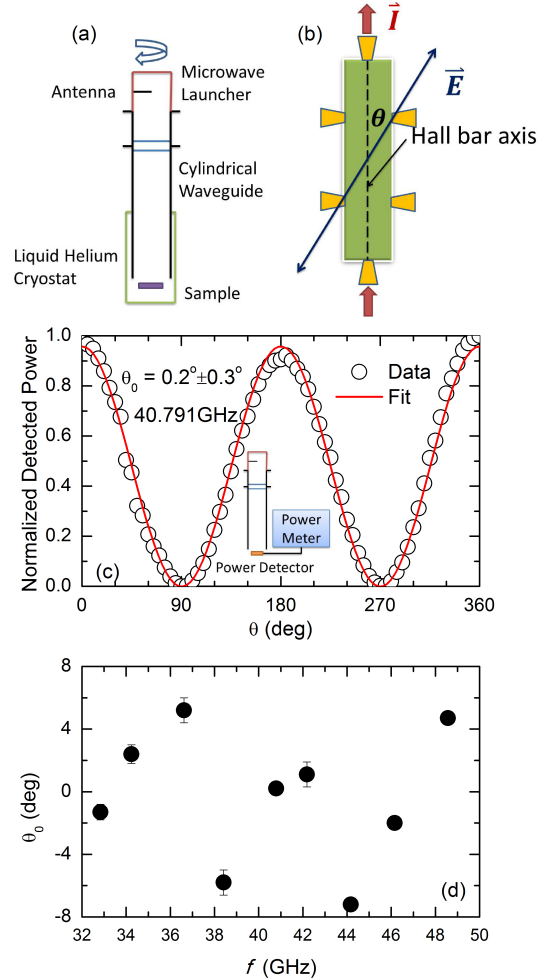


FIG. 1. (Color online) (a) Linearly polarized radiation generated by an antenna inside a rotatable microwave launcher is transmitted onto the specimen via a cylindrical waveguide. (b) This figure illustrates the orientation of the linearly polarized microwave radiation with respect to the specimen. θ is defined as the angle between the microwave electric field E and the Hall bar axis. (c) The sinusoidal normalized detected power as a function of θ , with a power detector in place of the sample, can be fit by a cosine square function in order to extract θ_0 . (d) A plot of θ_0 vs f , without the sample, implies that the measurement uncertainty in θ_0 is below $\approx 14^\circ$.

and Fig. 2(d) ($P1+^R$). Again, both of $P1+^L$ and $P1+^R$ are measured at the $P1+$ magnetic field, but from contact pairs on opposite sides of the Hall bar. The results show $\theta_0^L = 6.2^\circ \pm 0.6^\circ$ for $P1+^L$ and $\theta_0^R = -4.3^\circ \pm 0.5^\circ$ for $P1+^R$, where the small standard errors are due to the excellent fits to the cosine square function for oscillatory R_{xx} . The $\delta\theta_0 = |\theta_0^R - \theta_0^L| = 10.5^\circ \pm 0.8^\circ$ between $P1+^L$ and $P1+^R$, is less than the measurement uncertainty of 14° . Similarly, if we compare Fig. 2(e) ($V1+^L$) and (f) ($V1+^R$) or (g) ($P2+^L$) and (h) ($P2+^R$), the $\delta\theta_0 = 1.7^\circ \pm 1.6^\circ$ for $V1+$, and $\delta\theta_0 = 2.2^\circ \pm 0.5^\circ$ for $P2+$. These phase shift differences $\delta\theta_0$ are again smaller

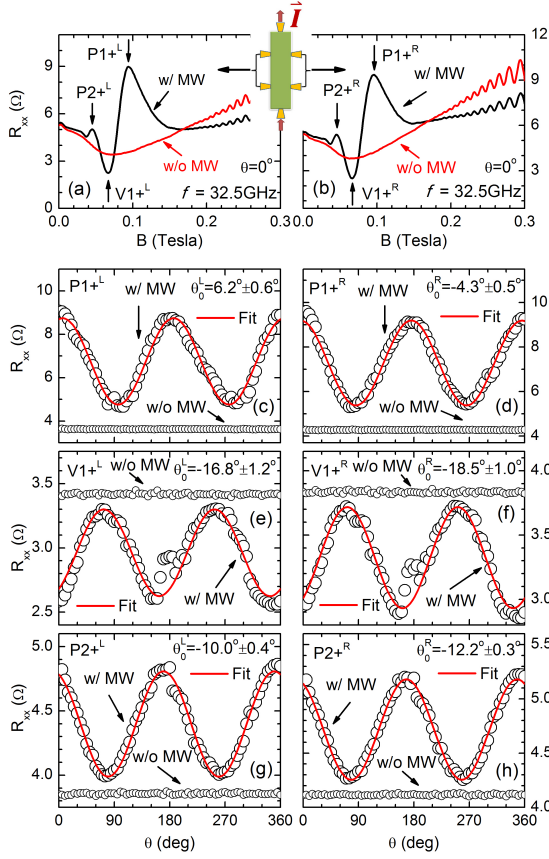


FIG. 2. (Color online) Panels (a) and (b) show R_{xx} with (photo-excited) and without (dark) microwave illumination for $0 \leq B \leq 0.3$ T, at $f = 32.5$ GHz and $\theta = 0$. Here, panel (a) shows the R_{xx} measured from the left (L) pair of contacts while panel (b) shows the R_{xx} measured from the right (R) pair of contacts on the Hall bar. Panels (c)-(h) exhibit oscillatory photo-excited and dark R_{xx} vs. the polarization angle θ , with extracted θ_0 obtained from the fit curve at (c) $P1+^L$ (d) $P1+^R$ (e) $V1+^L$ (f) $V1+^R$ (g) $P2+^L$ (h) $P2+^R$ respectively. Panels (c)-(h) show that the fit extracted θ_0 at a given extrema of the MIMOs have similar values for contact pairs on opposite sides ((L) and (R)) of the device with the phase shift difference being smaller than estimated measurement uncertainty ($\approx 14^\circ$).

than the measurement uncertainty.

Next, a comparison of the photo-excited and the dark R_{xx} vs B is shown in Fig. 3(a) and (b) for the same experimental parameters over the range $-0.3 \leq B \leq 0$ T. Similar to Fig. 2, R_{xx} measured on the left contact pair on the Hall bar is plotted in Fig. 3(a) (with superscript L), and that measured via right contact pair is shown in Fig. 3(b) (with superscript R). Three prominent extrema, which are now labeled as $P1-$, $V1-$ and $P2-$, represent the first peak, the first valley, and the second peak, respectively, for $B \leq 0$. Fig. 3(c)-(h) also exhibit traces of oscillatory photo-excited and dark R_{xx} vs θ at the $P1-L$, $P1-R$, $V1-L$, $V1-R$, $P2-L$, and $P2-R$ magnetic field values indicated in Fig. 3(a) and (b). The θ_0

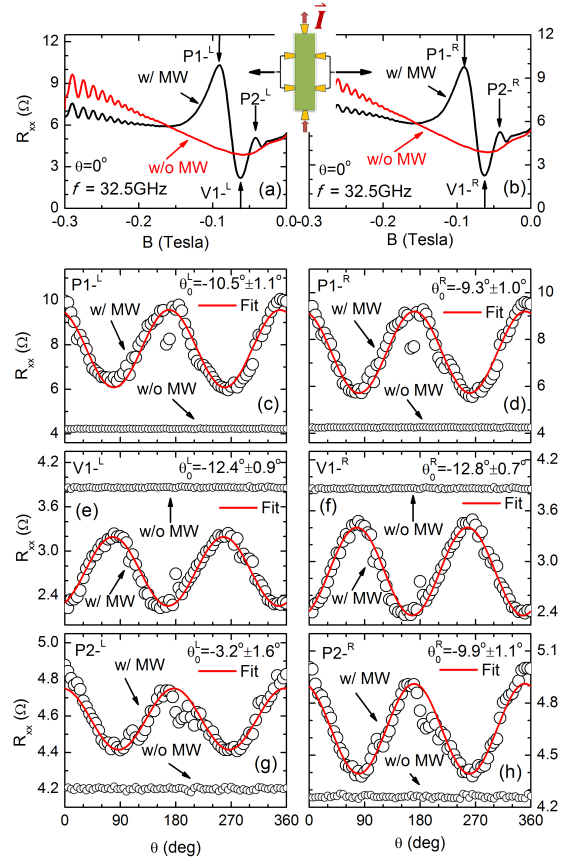


FIG. 3. (Color online) Panels (a) and (b) show R_{xx} with (photo-excited) and without (dark) microwave illumination for $-0.3 \leq B \leq 0$ T, at $f = 32.5$ GHz and $\theta = 0$. Here, panel (a) shows the R_{xx} measured from the left (L) pair of contacts while panel (b) shows the R_{xx} measured from the right (R) pair of contacts on the Hall bar. Panels (c)-(h) show oscillatory photo-excited and dark R_{xx} from the left-sided pair and the right-sided pair of contacts on the Hall bar, along with the extracted θ_0 at (c) $P1-L$ (d) $P1-R$ (e) $V1-L$ (f) $V1-R$ (g) $P2-L$ (h) $P2-R$, respectively. Panels (c)-(h) show that the fit extracted θ_0 at a given extrema of the MIMOs have similar values for contact pairs on opposite sides ((L) and (R)) of the device with the phase shift difference being smaller than estimated measurement uncertainty ($\approx 14^\circ$).

extracted by fitting the data to $R_{xx} = A \pm C \cos^2(\theta - \theta_0)$ are also displayed in Fig. 3 (c)-(h). As for the data of Fig. 2, we compare the θ_0 of opposite contact pairs at the extrema of RIMOs in the range of $B \leq 0$. At $P1-L$, $\theta_0^L = -10.5^\circ \pm 1.1^\circ$, and at $P1-R$, $\theta_0^R = -9.3^\circ \pm 1.0^\circ$, which yields $\delta\theta_0 = |\theta_0^R - \theta_0^L| = 1.2^\circ \pm 1.5^\circ$, still much smaller than the measurement uncertainty. For $V1-$ and $P2-$ (Fig. 3(e)-(h)), the $\delta\theta_0 = 0.4^\circ \pm 1.1^\circ$ and $\delta\theta_0 = 6.7^\circ \pm 1.9^\circ$, respectively, which are also within the estimated measurement uncertainty of $\approx 14^\circ$.

Similar results to those shown Fig. 2 and Fig. 3 for $f = 32.5$ GHz were observed at other microwave frequencies. That is, each $\delta\theta_0$ at these f were smaller than the measurement uncertainty. As a consequence, we make

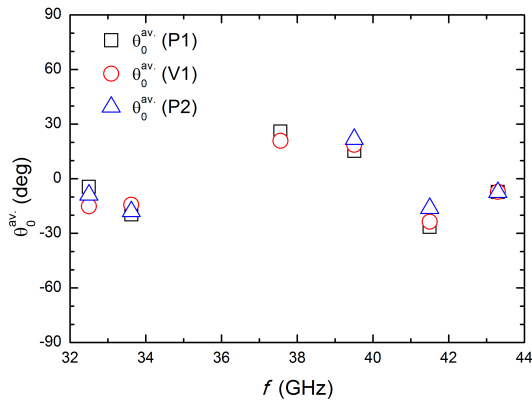


FIG. 4. (Color online) This panel shows a plot of the average value of θ_0 , i.e., $\theta_0^{av} = (\theta_0^+ + \theta_0^-)/2$ vs f for various extrema. The figure shows that θ_0^{av} for all extrema at a given f are close to each other. However, there is a large variation in θ_0^{av} with f .

the assumption that the θ_0 values obtained from the two opposite contact pairs at given B in this sample are practically indistinguishable. Thus, we average the θ_0^R and θ_0^L obtained from the opposite contact pairs of the Hall bar to reduce the measurement error in the extracted θ_0 , and assume that this average θ_0 is more representative of the corresponding sample area (see Fig. 1(b)). Table 1 provides a summary of the $\theta_0 = (\theta_0^R + \theta_0^L)/2$ obtained after averaging over opposite contact pairs. Here, θ_0^+ and θ_0^- are the θ_0 's for positive and negative magnetic fields, respectively.

For the sake of extracting the frequency dependence in θ_0 , we evaluate also θ_0^{av} , which is the average of θ_0^+ and θ_0^- . For example, $\theta_0^{av}(P1) = (\theta_0^+(P1) + \theta_0^-(P1))/2$, etc. The θ_0^{av} at the various extrema are shown in Fig. 4 as a function of f . Fig. 4 shows that the differences between any two of θ_0^{av} are less than 14° at each f . Further, the points appeared clustered at each f , and the point-clusters show a systematic variation with f . These results indicate a frequency dependence in the phase shift θ_0 even when a worst case scenario is applied for averaging over other smaller contributions to the phase shift.

III. DISCUSSION

From the results presented above, we suggest the following: (a) At low P , opposing contact pairs on a Hall bar present the same value for a given extremum, a given magnetic field direction, and a given f , for θ_0 that is extracted from the fit of $R_{xx}(\theta) = A \pm C \cos^2(\theta - \theta_0)$, within measurement uncertainty. (b) At a given f , the θ_0^{av} for all the considered extrema exhibit similar values, see Fig. 4. However, these values show a systematic dependence upon f .

Note that point (a) is expected since the two edges of the Hall bar are parallel to each other and their orientation with respect to the microwave polarization is the same. Since the GaAs/AlGaAs heterojunctions represent an extraordinarily clean system with mean-free paths approaching the mm- or sample size-scale, it is difficult to develop a scenario where the two edges of the homogeneous specimen would not exhibit the same linear polarization response. In this context it might be interesting to introduce non-parallel edges to see if that feature in the specimen introduces a phase shift in the response observed on the two edges. This will be a topic of future experiments.

Point (b) suggests that the magnitude of B does not produce profoundly distinguishable differences on representative θ_0 at the extrema of RIMOs in the specimen. The difference in this aspect between present and previous experimental work could be attributed to differences in sample quality and defect configuration within the specimen. From the theoretical perspective, Lei *et al.*⁶⁹ have simulated sinusoidal responses of R_{xx} as a function of polarization angle θ using the balance-equation formulation of their photon-assisted magneto-transport model. The results have indicated that the phase shift in the R_{xx} vs. θ response is dependent upon B or extremum, and f . Further, they suggested that $P1 + (\theta) = P1 - (\pi - \theta)$, $V1 + (\theta) = V1 - (\pi - \theta)$, etc. in an isotropic system, which is not observed here. However, it should be noted that real samples possibly include additional complexity, such as asymmetry, that was not considered in their theory.⁶⁹

Finally, although the cause of observed frequency-dependent θ_0 is not yet fully understood experimentally, and theory has not considered this possibility in our context, we draw a comparison with Faraday rotation in quantum Hall systems. In Faraday rotation, the polarization-plane of the transmitted linearly polarized radiation in the presence of magnetic field becomes a rotated by an angle, θ_F , which is called the Faraday angle. Generally, Faraday rotation, θ_F , is a function of radiation frequency per the Drude-Lorentz model⁷⁶⁻⁷⁸. The phase shifts θ_0 reported here appear, however, in a *dc* response, the magnetoresistance, observed under *ac*-excitation. One might qualitatively understand the observed θ_0 by suggesting that the 2DES rotates the polarization of the *ac* excitation, and the *dc* response then follows polarization of the rotated *ac* excitation. In such a situation, θ_0 could be a manifestation of θ_f . Further theory is needed, however, to provide more understanding of this possibility.

IV. CONCLUSION

The phase shifts observed in the polarization-angle-dependence of microwave-induced magnetoresistance oscillations have been processed using an analysis which emphasized averaging over the smaller contributions,

TABLE I. The representative θ_0^+ and θ_0^- at various f , at the extrema of RIMOs. Here, the superscripts '+' and '-' refer to positive and negative magnetic fields. θ_0^+ and θ_0^- at $f = 37.56$ for $P2$ are missing because these peaks were too small to be measured reliably. This comparison implies a given extremum under field reversal, shows similar θ_0 values for each f .

f (GHz)	θ_0^+ ($P1$)	θ_0^- ($P1$)	θ_0^+ ($V1$)	θ_0^- ($V1$)	θ_0^+ ($P2$)	θ_0^- ($P2$)
32.50	$1.0^\circ \pm 0.4^\circ$	$-9.9^\circ \pm 0.7^\circ$	$-17.7^\circ \pm 0.8^\circ$	$-12.6^\circ \pm 0.6^\circ$	$-11.1^\circ \pm 0.3^\circ$	$-6.6^\circ \pm 1.0^\circ$
33.62	$-12.5^\circ \pm 0.6^\circ$	$-26.8^\circ \pm 0.6^\circ$	$-11.2^\circ \pm 0.5^\circ$	$-17.5^\circ \pm 0.9^\circ$	$-14.0^\circ \pm 0.4^\circ$	$-22.0^\circ \pm 0.8^\circ$
37.56	$25.1^\circ \pm 0.4^\circ$	$26.7^\circ \pm 0.5^\circ$	$25.0^\circ \pm 0.5^\circ$	$16.7^\circ \pm 0.5^\circ$	–	–
39.51	$16.3^\circ \pm 0.6^\circ$	$14.3^\circ \pm 0.8^\circ$	$11.7^\circ \pm 1.1^\circ$	$25.7^\circ \pm 0.9^\circ$	$18.4^\circ \pm 0.7^\circ$	$25.1^\circ \pm 0.8^\circ$
41.50	$-32.5^\circ \pm 0.6^\circ$	$-20.5^\circ \pm 0.4^\circ$	$-23.3^\circ \pm 1.0^\circ$	$-23.8^\circ \pm 1.0^\circ$	$-18.5^\circ \pm 1.8^\circ$	$-14.0^\circ \pm 0.6^\circ$
43.30	$-11.7^\circ \pm 0.3^\circ$	$-2.7^\circ \pm 0.5^\circ$	$-11.1^\circ \pm 0.8^\circ$	$-3.2^\circ \pm 1.9^\circ$	$-14.3^\circ \pm 0.9^\circ$	$-0.6^\circ \pm 0.9^\circ$

when the smaller contributions were smaller than estimates of the experimental uncertainty. The analysis was carried out in order to extract a possible microwave frequency contribution to the phase shift, $\theta_0(f)$, observed in the R_{xx} vs. θ response of the microwave radiation-induced magnetoresistance oscillations. The analysis demonstrates a non-vanishing frequency dependent contribution to the phase shift over the frequency interval $32 \leq f \leq 50$ GHz.

V. ACKNOWLEDGE

Magnetotransport studies and T.Ye at Georgia State University were supported by the US Department of Energy, Office of Basic Energy Sciences, Material Sciences and Engineering Division under DE-SC001762. H.-C. Liu was supported by the ARO under W911NF-10-1-0450.

- ¹R. G. Mani, J. H. Smet, K. von Klitzing, V. Narayanamurti, W. B. Johnson, and V. Umansky, Nature (London) **420**, 646 (2002).
- ²M. A. Zudov, R. R. Du, L. N. Pfeiffer, and K. W. West, Phys. Rev. Lett. **90**, 046807 (2003).
- ³P. H. Siegel, IEEE Trans. Microwave Theory and Techniques, **50**, 910-928 (2002).
- ⁴B. B. Hu and M. C. Nuss, Optics Lett. **20**, 1716-1718 (1995).
- ⁵R. G. Mani, Appl. Phys. Lett. **92**, 102107 (2008).
- ⁶R. G. Mani, V. Narayanamurti, K. von Klitzing, J. H. Smet, W. B. Johnson and V Umansky, Phys. Rev. B **69**, 161306(R) (2004); Phys. Rev. B **70**, 155310 (2004).
- ⁷R. G. Mani, J. H. Smet, K. von Klitzing, V. Narayanamurti, W. B. Johnson and V. Umansky, Phys. Rev. Lett. **92**, 146801 (2004); Phys. Rev. B **69**, 193304 (2004).
- ⁸S. A. Studenikin, M. Potemski, P. T. Coleridge, A. S. Sachrajda and Z. R. Wasilewski, Solid State Commun. **129**, 341-345 (2004).
- ⁹R. G. Mani, Physica E (Amsterdam) **22**, 1-6 (2004); Physica E Amsterdam **25**, 189-197 (2004); Int. J. Mod. Phys. B **18**, 3473-3480 (2004); Appl. Phys. Lett. **85**, 4962-4964 (2004); Phys. Rev. B **72**, 075327 (2005); Z. Phys. B **92**, 335 (1993); J. Phys. Soc. Jpn. **65**, 1751 (1996); Appl. Phys. Lett. **91**, 132103 (2007); Solid State Comm. **144**, 409-412 (2007); Physica E (Amsterdam) **40**, 1178-1181 (2008).
- ¹⁰A. E. Kovalev, S. A. Zvyagin, C. R. Bowers, J. L. Reno and J. A. Simmons, Solid State Commun. **130**, 379-381 (2004).
- ¹¹R. R. Du, M. A. Zudov, C. L. Yang, L. N. Pfeiffer and K. W. West, Physica E **22**, 7-12 (2004).
- ¹²J. H. Smet, B. Gorshunov, C. Jiang, L. Pfeiffer, K. West, V. Umansky, M. Dressel, R. Meisels, F. Kuchar and K. von Klitzing, Phys. Rev. Lett. **95**, 116804 (2005).
- ¹³A. Wirthmann, B. D. McCombe, D. Heitmann, S. Holland, K. Friedland and C.-M. Hu, Phys. Rev. B **76**, 195315 (2007).
- ¹⁴S. A. Studenikin, A. S. Sachrajda, J. A. Gupta, Z. R. Wasilewski, O. M. Fedorych, M. Byszewski, D. K. Maude, M. Potemski, M. Hilke, K. W. West and L. N. Pfeiffer, Phys. Rev. B **76**, 165321 (2007).
- ¹⁵O. E. Raichev, Phys. Rev. B **78**, 125304 (2008).
- ¹⁶S. Wiedmann, G. M. Gusev, O. E. Raichev, T. E. Lamas, A. K. Bakarov and J. C. Portal, Phys. Rev. B **78**, 121301(R) (2008).
- ¹⁷R. G. Mani, W. B. Johnson, V Umansky, V. Narayanamurti and K. Ploog, Phys. Rev. B **79**, 205320 (2009).
- ¹⁸L.-C. Tung, C. L. Yang, D. Smirnov, L. N. Pfeiffer, K. W. West, R. R. Du and Y.-J. Wang, Solid State Commun. **149**, 1531-1534 (2009).
- ¹⁹R. G. Mani, C. Gerl, S. Schmult, W. Wegscheider and V. Umansky, Phys. Rev. B **81**, 125320 (2010).
- ²⁰A. N. Ramanayaka and R. G. Mani, Phys. Rev. B **82**, 165327 (2010).
- ²¹S. Wiedmann, G. M. Gusev, O. E. Raichev, A. K. Bakarov and J. C. Portal, Phys. Rev. B **81**, 085311 (2010).
- ²²O. M. Fedorych, M. Potemski, S. A. Studenikin, J. A. Gupta, Z. R. Wasilewski and I. A. Dmitriev, Phys. Rev. B **81**, 201302(R) (2010).
- ²³S. Wiedmann, G. M. Gusev, O. E. Raichev, A. K. Bakarov and J. C. Portal, Phys. Rev. Lett. **105**, 026804 (2010).
- ²⁴A. N. Ramanayaka, R. G. Mani and W. Wegscheider, Phys. Rev. B **83**, 165303 (2011).
- ²⁵R. G. Mani, A. N. Ramanayaka and W. Wegscheider, Phys. Rev. B **84**, 085308 (2011).
- ²⁶A. N. Ramanayaka, R. G. Mani, J. Iñarrea and W. Wegscheider, Phys. Rev. B **85**, 205315 (2012).
- ²⁷A. Bogani, A. T. Hatke, S. A. Studenikin, A. Sachrajda, M. A. Zudov, L. N. Pfeiffer and K. W. West, Phys. Rev. B **86**, 235305 (2012).
- ²⁸R. G. Mani, J. Hankinson, C. Berger and W. A. de Heer, Nat. Commun. **3**, 996 (2012).
- ²⁹S. Dietrich, S. Byrnes, S. Vitkalov, A. V. Goran and A. A. Bykov, J. Appl. Phys. **113**, 053709 (2013).
- ³⁰R. G. Mani, A. N. Ramanayaka, T. Ye, M. S. Heimbeck, H. O. Everitt and W. Wegscheider, Phys. Rev. B **87**, 245308 (2013).
- ³¹R. G. Mani, A. Kriisa and W. Wegscheider, Sci. Rep. **3**, 2747 (2013).
- ³²R. G. Mani and A. Kriisa, Sci. Rep. **3**, 3478 (2013).
- ³³T. Ye, R. G. Mani and W. Wegscheider, Appl. Phys. Lett. **102**, 242113 (2013); *ibid* **103**, 192106 (2013); *ibid* **105**, 191609 (2014).
- ³⁴A. T. Hatke, M. A. Zudov, J. D. Watson, M. J. Manfra, L. N. Pfeiffer and K. W. West, Phys. Rev. B **87**, 161307(R) (2013).
- ³⁵D. Konstantinov, Y. Monarkha and K. Kono, Phys. Rev. Lett. **111**, 266802 (2013).
- ³⁶T. Ye, H.-C. Liu, W. Wegscheider and R. G. Mani, Phys. Rev. B **89**, 155307 (2014).
- ³⁷A. C. Durst, S. Sachdev, N. Read and S. M. Girvin, Phys. Rev. Lett. **91**, 086803 (2003).

- ³⁸V. Ryzhii and R. Suris, *J. Phys.: Condens. Matter* **15**, 6855-6869 (2003).
- ³⁹X. L. Lei and S. Y. Liu, *Phys. Rev. Lett.* **91**, 226805 (2003).
- ⁴⁰A. A. Koulakov and M. E. Raikh, *Phys. Rev. B* **68**, 115324 (2003).
- ⁴¹A. V. Andreev and I. L. Aleiner and A. J. Millis, *Phys. Rev. Lett.* **91**, 056803 (2003).
- ⁴²V. Ryzhii, *Phys. Rev. B* **68**, 193402 (2003).
- ⁴³X. L. Lei, *J. Phys.: Condens. Matter* **16**, 4045-4060 (2004).
- ⁴⁴K. Park, *Phys. Rev. B* **69**, 201301(R) (2004).
- ⁴⁵P. H. Rivera and P. A. Schulz, *Phys. Rev. B* **70**, 075314 (2004).
- ⁴⁶S. A. Mikhailov, *Phys. Rev. B* **70**, 165311 (2004).
- ⁴⁷A. Auerbach, I. Finkler, B. I. Halperin and Amir Yacoby, *Phys. Rev. Lett.* **94**, 196801 (2005).
- ⁴⁸J. Iñarrea and G. Platero, *Phys. Rev. Lett.* **94**, 016806 (2005).
- ⁴⁹X. L. Lei and S. Y. Liu, *Phys. Rev. B* **72**, 075345 (2005).
- ⁵⁰I. A. Dmitriev, M. G. Vavilov, I. L. Aleiner, A. D. Mirlin and D. G. Polyakov, *Phys. Rev. B* **71**, 115316 (2005).
- ⁵¹J. Iñarrea and G. Platero, *Appl. Phys. Lett.* **89**, 052109 (2006).
- ⁵²J. Dietel, *Phys. Rev. B* **73**, 125350 (2006).
- ⁵³J. Iñarrea and G. Platero, *Phys. Rev. B* **76**, 073311 (2007).
- ⁵⁴A. D. Chepelianskii, A. S. Pikovsky and D. L. Shepelyansky, *Eur. Phys. J. B* **60**, 225-229 (2007).
- ⁵⁵J. Iñarrea and G. Platero, *Phys. Rev. B* **78**, 193310 (2008).
- ⁵⁶J. Iñarrea and G. Platero, *Appl. Phys. Lett.* **93**, 062104 (2008).
- ⁵⁷S. Wang and T.-K. Ng, *Phys. Rev. B* **77**, 165324 (2008).
- ⁵⁸J. Iñarrea and G. Platero, *Appl. Phys. Lett.* **95**, 162106 (2009).
- ⁵⁹I. G. Finkler and B. I. Halperin, *Phys. Rev. B* **79**, 085315 (2009).
- ⁶⁰P. H. Rivera, A. L. C. Pereira and P. A. Schulz, *Phys. Rev. B* **79**, 205406 (2009).
- ⁶¹X. L. Lei and S. Y. Liu, *Appl. Phys. Lett.* **94**, 232107 (2009).
- ⁶²J. Iñarrea and G. Platero, *Nanotechnology* **21**, 315401 (2010).
- ⁶³Jesús Iñarrea, R. G. Mani and W. Wegscheider, *Phys. Rev. B* **82**, 205321 (2010).
- ⁶⁴J. Iñarrea and G. Platero, *Phys. Rev. B* **84**, 075313 (2011).
- ⁶⁵J. Iñarrea, *Appl. Phys. Lett.* **99**, 232115 (2011).
- ⁶⁶S. A. Mikhailov, *Phys. Rev. B* **83**, 155303 (2011).
- ⁶⁷A. D. Chepelianskii, J. Laidet, I. Farrer, H. E. Beere, D. A. Ritchie and H. Bouchiat, *Phys. Rev. B* **86**, 205108 (2012).
- ⁶⁸J. Iñarrea, *Appl. Phys. Lett.* **100**, 242103 (2012).
- ⁶⁹X. L. Lei and S. Y. Liu, *Phys. Rev. B* **86**, 205303 (2012).
- ⁷⁰J. Iñarrea, *Phys. Lett. A* **377**, 2642 (2013).
- ⁷¹J. Iñarrea, *J. Appl. Phys.* **113**, 183717 (2013).
- ⁷²A. Kunold and M. Torres, *Physica B* **425**, 78-82 (2013).
- ⁷³O. V. Zhironov, A. D. Chepelianskii and D. L. Shepelyansky, *Phys. Rev. B* **88**, 035410 (2013).
- ⁷⁴J. Iñarrea, *Europhys. Lett.* **106**, 47005 (2014).
- ⁷⁵X. L. Lei and S. Y. Liu, *J. Appl. Phys.* **115**, 233711 (2014).
- ⁷⁶Iris Crassee, Julien Levallois, Andrew L. Walter, Markus Ostler, Aaron Bostwick, Eli Rotenberg, Thomas Seyller, Dirk van der Marel and Alexey B. Kuzmenko, *Nat. Phys.* **7**, 48-51 (2011).
- ⁷⁷A. M. Shuvaev, G. V. Astakhov, A. Pimenov, C. Brne, H. Buhmann and L. W. Molenkamp, *Phys. Rev. Lett.* **106**, 107404 (2011).
- ⁷⁸R. Shimano, G. Yumoto, J. Y. Yoo, R. Matsunaga, S. Tanabe, H. Hibino, T. Morimoto and H. Aoki, *Nat. Commun.* **4**, 1841 (2013).